Journal of Applied Geophysics 125 (2016) 45–55

Contents lists available at ScienceDirect

Journal of Applied Geophysics

journal homepage: www.elsevier.com/locate/jappgeo

Adaptive sampling of AEM transients

Domenico Di Massa [a,*], Giovanni Florio [a], Andrea Viezzoli [b]

[a] Department of Earth, Environment and Resources Sciences, University of Naples Federico II, Largo San Marcellino 10, 80138 Naples, (Italy)
[b] Aarhus Geophysics Aps, C.F. Møllers Alle 4, Aarhus C 8000, Denmark

ARTICLE INFO

Article history:
Received 5 May 2015
Received in revised form 9 December 2015
Accepted 5 January 2016
Available online 9 January 2016

Keywords:
Airborne electromagnetics
Time domain electromagnetics
Transient sampling
Adaptive-gating
Sensitivity

ABSTRACT

This paper focuses on the sampling of the electromagnetic transient as acquired by airborne time-domain electromagnetic (TDEM) systems.
Typically, the sampling of the electromagnetic transient is done using a fixed number of gates whose width grows logarithmically (log-gating). The log-gating has two main benefits: improving the signal to noise (S/N) ratio at late times, when the electromagnetic signal has amplitudes equal or lower than the natural background noise, and ensuring a good resolution at the early times. However, as a result of fixed time gates, the conventional log-gating does not consider any geological variations in the surveyed area, nor the possibly varying characteristics of the measured signal.
We show, using synthetic models, how a different, flexible sampling scheme can increase the resolution of resistivity models. We propose a new sampling method, which adapts the gating on the base of the slope variations in the electromagnetic (EM) transient.
The use of such an alternative sampling scheme aims to get more accurate inverse models by extracting the geoelectrical information from the measured data in an optimal way.

1. Introduction

Time-domain airborne electromagnetic data are regularly acquired over wide areas for various applications such as groundwater, environmental and mining exploration (e.g. Fitterman, 1987; Auken et al., 2003; Reid and Viezzoli, 2007; Viezzoli et al., 2010; Podgorski et al., 2013). The modeling of these data is often aimed at obtaining a quantitative estimation of the 3D spatial distribution of the conductivity of the earth, through an inversion process. The obtained model may be used for further geological or hydrogeological interpretations.

The electromagnetic (EM) secondary field is measured as a function of time using an induction coil.

In TDEM, the decay over time of the secondary magnetic field associated to the induced currents is recorded in time-windows, called gates.

The width of the gates is a crucial factor in the acquisition of electromagnetic data. In fact, it controls two signal features that strongly influencing the inversion results: the data signal to noise (S/N) ratio and the capacity of resolving the structure in the subsurface (resolution).

In general, the S/N ratio increases with the gates width in contrast the resolution capability is better for smaller gates that provide more details on specific parts of EM decay and will be necessarily noisier than larger gates (Nabighian and Macnae, 1991). A correct sampling must take into account the trade-off between these two components.

The "gating", i.e., the sampling in time of the secondary field, is often chosen following a standard approach, using the same number of gates per time decade with a logarithmic increase of the width with time in order to improve S/N ratio (log-gating) (Munkholm and Auken, 1996).

Nowadays, thanks to technological advancements, new airborne systems are able to measure and record the secondary field at high sampling rate, yielding a virtually continuous stream of data. In this paper, the attention is focused on the binning of the streamed transients. We will show, using synthetic models, how different sampling schemes can influence the results of the inversion.

The processing of small width gates is complicated by high noise levels. It can therefore be difficult and the inversion of large amount of gates is very time consuming. An average of measurements (binning) over windows of finite width is usually necessary.

We propose a new sampling method that consists in adapting the gating on the base of the slope variations in the EM transient sampled at the highest possible frequency (the so called streamed data). As the EM transient decay depends on the distribution of the conductivity at depth in the sensitive area (footprint), there are some time intervals in the EM transient that contain more information on the subsurface structures. Our idea is to extract these information from measured data with an optimized sampling, in order to get more accurate inverse models.

* Corrisponding author at: Department of Earth, Environment and Resources Sciences, University of Naples Federico II, Largo San Marcellino 10, 80138 Naples, Italy.
E-mail address: domenico.dimassa@unina.it (D. Di Massa).

http://dx.doi.org/10.1016/j.jappgeo.2016.01.002
0926-9851/

2. Methodology

The time variation of the secondary magnetic field, measured as db/dt at an induction receiver coil, exhibits, at late times, a decay proportional to $t^{-5/2}$ in a log–log plot for a homogeneous half-space (Christiansen et al., 2009).

$$\frac{\partial b_z}{\partial t} \approx \left(\frac{M}{20}\right)\left(\frac{\sigma}{\pi}\right)^{\frac{3}{2}}\left(\frac{\mu_0}{t}\right)^{\frac{5}{2}} \quad (1)$$

where M is the magnetic moment of the transmitter (Am^2), σ is the conductivity (S/m) and μ_0 is the magnetic permeability of the free-space (H/m).

At the interface of two layers with different conductivity, the value of the secondary field changes according to the variation of the conductivity as shown in Formula 1.

This means that for a horizontally layered model, the transient decay, $(\partial b_z/\partial t)$, shows a slope variation in corresponding to the transition between two layers with different conductivity.

Fig. 1 (from Christiansen et al., 2009) shows the EM transient for a homogeneous half-space with varying resistivities. The response of a two-layer earth having a resistivity of 100 Ωm in layer 1 and 10 Ωm in layer 2, and with the thickness of layer 1 of 40 m, is also shown.

The slope variations are related to the conductivity contrast between two electro-layers.

The conductivity controls also the diffusion speed of the current in the ground:

$$v = 2(\pi\sigma\mu t)^{-1/2} \quad (2)$$

where σ and μ are the conductivity (S/m) and the relative magnetic permeability (H/m) of the medium and t is the time (s).

The diffusion speed decreases when going through conductive layers. Formula 1 and 2 explain why the TDEM method is highly sensitive to conductivity layers (Telford et al., 1990).

The analysis of noise-free data produced by simple two-layer models and calculated from the solution of 1D forward model (Ward and Hohmann, 1988) shows that the transition from a conductive layer to a resistive one corresponds to a minimum in the second time derivative of the transient. On the contrary, the transition from a resistive layer to a conductive one shows a maximum of curvature. In Fig. 2a the EM transient (blue curve) and the curvature (green curve) for two-layer earth with 50 Ωm in layer 1 and 10 Ωm in layer 2, with the thickness of layer 1 of 50 m, are shown. In Fig. 2b, we plotted the same quantities when the conductive layer is the shallowest.

The decay of the electromagnetic transient is measured as average response over time windows of finite width (gates). As we already mentioned, the modern airborne EM systems are able to measure the secondary field with digital receivers recording the full decay stream at high sampling rate. As it is difficult to manage the processing of large amount of small width gates for which the signal to noise ratio is considerably lower and the inversion of many gates can be time consuming, the time binning of the acquisition data is necessary.

Typically, the sampling of the electromagnetic transient is done using a fixed number of gates whose width grows logarithmically (LOG-GATING). The log-gating has two main benefits: improving the S/N ratio at late times, when the electromagnetic signal has amplitudes equal or lower than the natural background noise, and at the same time ensuring a good resolution at the early times.

It is clear that in order to obtain correct models, a good sampling of the EM transient is needed. We demonstrate the previous statement by illustrating how the inversion result changes when EM transient is undersampled in various ways (Fig. 3). In these tests, we used noise-free data, calculated from the solution of the 1D forward problem (Ward and Hohmann, 1988) for a four layer model. We used 21 gates in log-gating configuration and inverted the data using AarhusInv

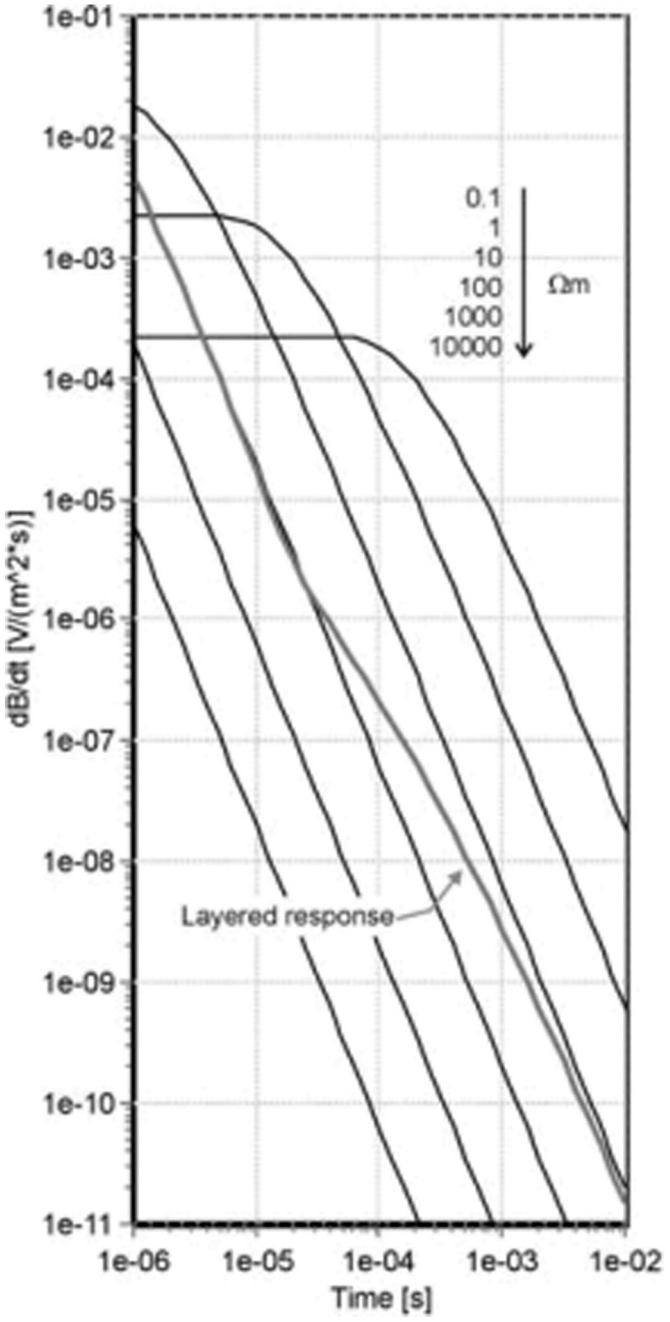

Fig. 1. Transient responses for a homogeneous half-space with varying resistivities and for a layered half-space (from Christiansen et al., 2009).

inversion code (Kirkegaard and Auken, 2015), removing a group of three adjacent gates. The starting model is a layered halfspace with a resistivity of 90 Ωm. Being noise-free data, the inversion should (or rather could, depending on the sampling scheme) recover a useful model.

The analysis of the results illustrated in Fig. 3, shows that removing the information carried by even a small number of data (gates) causes a loss of resolution, with inaccuracies on both conductivity and thickness in the computed inverse models.

However, the worst models are obtained when the removed gates are in correspondence with the maxima and the minima of curvature that, as shown in Fig. 2, mark the transition between two layers. In fact, from the curvature of the EM transient in Fig. 3a we note the presence of two minima in the first and the third decade and one maximum in the second decade. Undersampling the transient in correspondence of the minimum of the first decade does not affect the inversion results

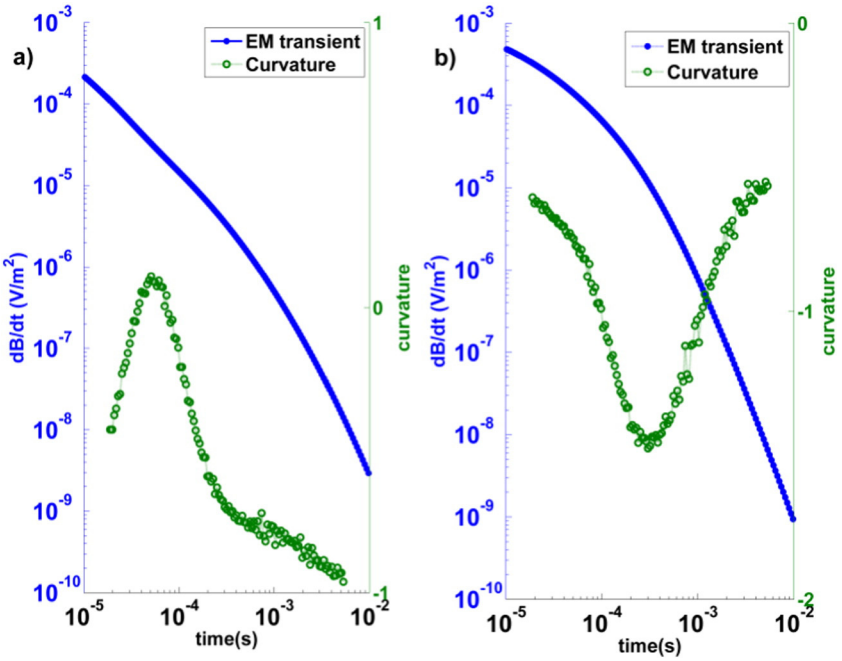

Fig. 2. EM transient (blue curve) and its curvature (green curve) for two-layers model earth with a resistive layer of 50 Ωm and a conductive one of 10 Ωm, the thickness of shallowest layer being 50 m. (a) The resistive layer is the shallowest. (b)The conductive layer is the shallowest. (For interpretation of the references to color in this figure legend, the reader is referred to the web version of this article.)

more than removing other gates of this decade. However, by removing the gates that are in correspondence with the maximum and the minimum of curvature in the second and third decade (from 11th to 17th), the recovered models are less accurate in the definition of the thickness and resistivity of the electro-layers. This confirms that there are some time intervals in the EM transient decay that contain more information on the structures in the subsurface.

Thus, we propose a new approach to sample the EM transient that we call adaptive gating.

Our method simply consists in a more detailed sampling of the time intervals at which the electromagnetic response shows the greater sensitivity to the changes of resistivity of the subsurface. The second derivative of the EM transient is the base for our adaptive-gating.

In Fig. 3, we notice, in fact, that the gates from the 10th to the 13th match clearly with the maximum of curvature, and thus can be easily identified also in a real signal. On the contrary, gates from the 13th to the 17th are only partially in correspondence to a minimum of curvature. Similar observations were drawn on a series of synthetic studies with different 1D models.

We extensively tested our adaptive-gating procedure for the maxima and for the minima of curvature arising from four-layer models. We noticed that the most correct inversion results are those obtained adapting the gating only for maxima of the curvature.

This is hardly surprising, as it is in this case that the EM methods have most resolution power, as opposed to a transition towards higher resistivities. We conclude that the crucial parts of the transient that require customized gating are those in correspondence to the maxima of curvature, which marks the transition from a resistive layer to a conductive one. According to this strategy, the gate-width at the maximum of the curvature is reduced, while we progressively increase the widths of the gates at the sides of the identified maximum.

This scheme should guarantee a better resolution for the most informative part of the signal that, according to the velocity propagation and the density of the currents, is in correspondence of the conductive layers.

To demonstrate the benefits of such a sampling scheme of the EM transient, we present now a series of tests on synthetic data where we compare the inversion models obtained with the 'classical' log-gating and our adaptive-gating approaches.

To perform these tests, we:

- simulated a continuous acquisition of the EM transient decay. The parameters of the electromagnetic airborne system are listed in Table 1;
- defined a 1D model of electro-layers, defined by thicknesses and conductivities;
- added a noise to the data based on the model by Munkholm and Auken (1996);
- applied a denoising filter through the Discrete Wavelet Transform (DWT; Fedi and Quarta, 1998);
- computed the second derivatives of the EM transient to identify the most sensitive time intervals;
- sampled the continuous acquisition data using both log-gating and adaptive-gating schemes;
- inverted the two data sets and compared the results.

We simulated a continuous acquisition by using 147 gates having a width increasing logarithmically in the range between 10^{-5} and 10^{-2} s.

Then, the solution of the 1D forward problem was computed (Ward and Hohmann, 1988) for each considered model.

The forward response was perturbed with a random noise. We used the model noise proposed by Munkholm and Auken (1996). Following this approach, the noise is approximated to a straight line with slope equal to $-1/2$ in a log–log plot, with a value of 3 nV/m^2 at 1 ms.

The second derivative is computed in the time domain by simple finite differences relations.

Then, to find the most sensitive time intervals needed to implement the sampling with our adaptive-gating scheme, the maxima of the curvature of the EM transient were investigated. However, the noise on the data prevents the reliable identification of these time intervals. Thus, data must be first denoised. Among various techniques, we chose to low-pass filter using the Discrete Wavelet Transform (DWT; Fedi and Quarta, 1998). In the wavelet domain, the scales may be associated with the frequency: small scales are in connection with high-frequency

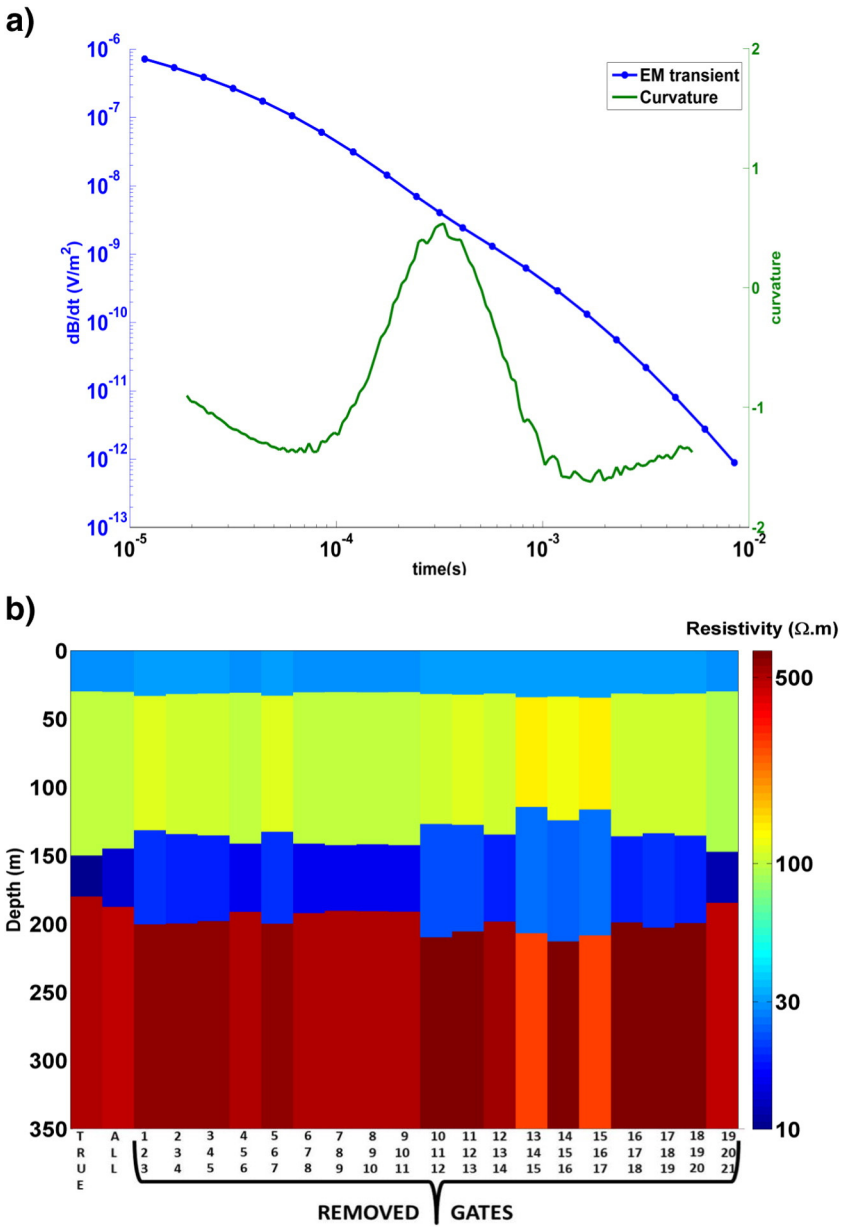

Fig. 3. (a) The EM transient (blue curve) sampled with 21 gates in log-gating configuration and its curvature (green curve). (b) The inverse models, obtained by removing different groups of three adjacent gates, are compared with the true model ("TRUE" column) and with that obtained using all the available gates ("ALL" column). (For interpretation of the references to color in this figure legend, the reader is referred to the web version of this article.)

components of the signal and large scales with those at low frequency. Thanks to the characteristics of the DWT to provide a time-scale approximation of the analyzed signal, it is possible to perform a localized denoising, that is filtering certain frequencies only at some times leaving intact the rest of the signal.

Table 1
Parameters of the electromagnetic airborne system used in the simulation.

Secondary field	dB/dt (V/m^2), vertical component Z
Flying height	30 m
Magnetic moment	160,000 Am^2
On-time	7000 μs, trapezoidal waveform
Off-time	13,000 μs
Ramp-on	4000 μs
Ramp-off	100 μs
Low pass filter	100 kHz

Fig. 4 shows the effect of the DWT on one of the transients (Fig. 4a). The DWT filtering includes a multiresolution analysis of the signal (Fig. 4b). In this case the EM transient is decomposed in 7 details at different scale and a low resolution approximation of the signal (black line on the upper part of the multiresolution graph, Fig. 4).

The noise gives evidence on different scales, and especially on the scales with number −4, −5, −6 and −7 and from 110th sample that represents the point when the EM transient drops into the noise. To remove it we set the coefficients to zero of the DWT corresponding to these scales (Fig. 4d), and the filtered signal (Fig. 4c) was then reconstructed using the details from −1 to −3. The residual signal (Fig. 4e) shows that the filtering acts for the entire transient and especially where the effects of noise become dominant on the secondary field.

After the filtering of the EM transient, we identified the most sensitive time intervals and we sampled the data of the continuous acquisition using 21 gates by both the adaptive-gating and log-gating schemes.

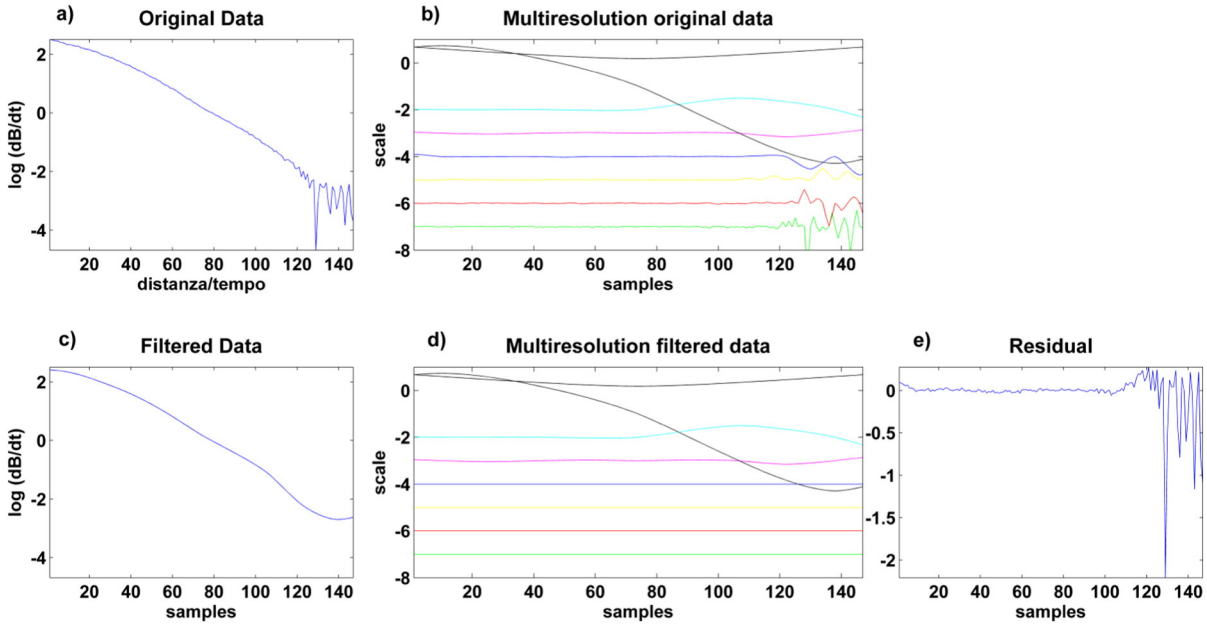

Fig. 4. DWT filtering on EM transient. (a) Original EM transient. (b) Multiresolution of the original data. (c) Filtered EM transient. (d) Multiresolution of the filtered data. (e) Residual filtering.

The last step was the 1D inversion with AarhusInv inversion code (Kirkegaard and Auken, 2015) of these data and the comparison of the resulting models. We want to stress here that no filtering were applied to data prior to the inversion. We used the DWT filtering only to identify the time intervals (maxima of curvature) where to adapting the gating.

3. Results

We first tested our approach on synthetic TDEM data obtained from two different individual 4 layers models. The first four-layer model has a third conductive layer between two resistive layers (Fig. 5a).

The second four-layer model has a third resistive layer between two conductive layers (Fig. 5b).

Then we moved to a more complex structure that could be representative of a buried valley model.

The buried valley model consists in a series of 52 four-layer models, with a thickness variation of the second resistive layer (Fig. 12a).

Below we will show all the steps of the application of our approach for the two four-layer models. The same steps were followed also for every sounding of the buried valley model, even if we will show only the final results.

3.1. Four-layer models

First, we calculated the forward response for the considered model using 147 logarithmically spaced gates in time interval between 10^{-5} to 10^{-2} s. The center time of the first gate is 1.2×10^{-5} s and the center time of the last gate is 9.8×10^{-3} s. The data were perturbed with a random noise and we calculated the curvature of the EM transient (Fig. 6).

The noise in the data is strongly enhanced in the second derivative of the EM transient and makes it impossible any reliable identification of the most representative maxima of the curvature. A denoising filter is then applied to emphasize those time intervals at which the gate widths reduce or enlarge following the adaptive-gating scheme. The DWT proved to be a suitable low-pass filtering technique. As we are dealing with synthetic data, we could compare the filtering results with those achieved with noise-free data and we verified that the positions in time of our maxima of curvature in the filtered data were the same of noise-free data (Fig. 7).

We computed the second derivative of the filtered EM transient and could easily identify the time intervals corresponding to the maxima (Fig. 8), marking the transition from data mostly influenced by the upper resistive layer to those mostly influenced by the below conductive one. The identification of the maxima was performed by considering

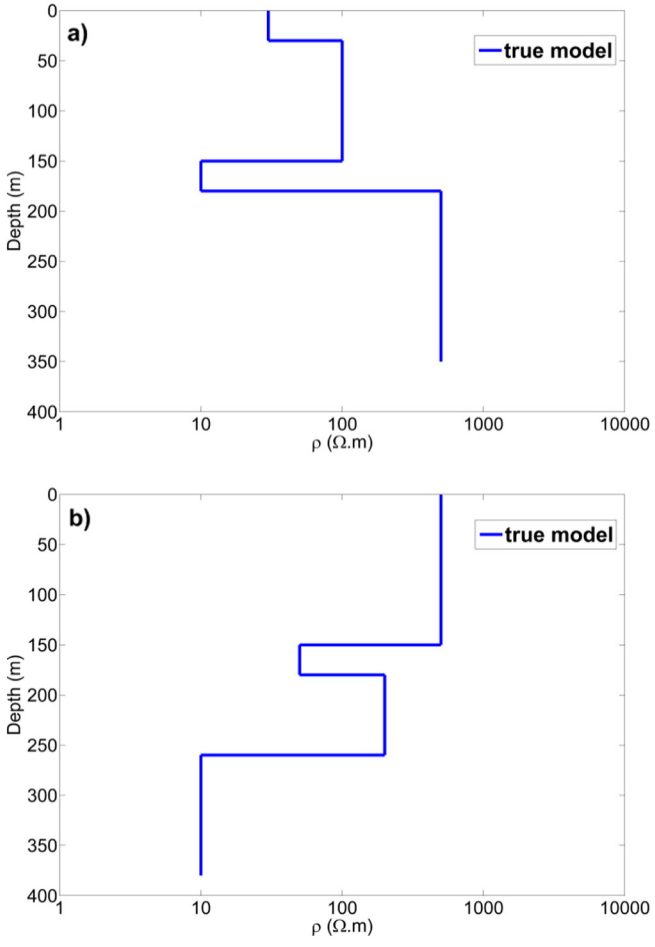

Fig. 5. (a) Four-layer model with a third conductive layer between two resistive layers; (b) four-layer model with a third resistive layer between two conductive layers.

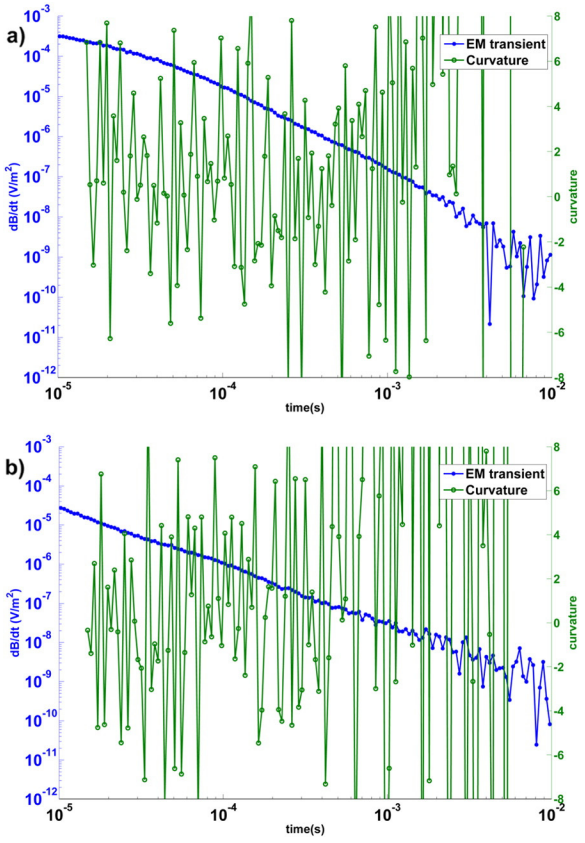

Fig. 6. (a) EM transient (blue curve) and its curvature (green curve) for the first four-layer model earth; (b) EM transient (blue curve) and its curvature (green curve) for the second four-layer model earth. (For interpretation of the references to color in this figure legend, the reader is referred to the web version of this article.)

only those having a great amplitude (at 3×10^{-4} s in Fig. 8a; at 3×10^{-5} and at 3×10^{-4} s in Fig. 8b) and discarding minor oscillations of the second derivative (at 6.7×10^{-4} s in Fig. 8a; at 7.7×10^{-5} s and 7×10^{-4} in Fig. 8b). Moreover, we excluded maxima at the late times, when the S/N ratio is evidently low.

Then we sampled the data according to the adaptive-gating and log-gating schemes, by defining the center and the width of 21 gates. The adaptive-gating approach was different from the 'classical' log-gating scheme in that we sampled the EM transient by reducing the gate-width at the time corresponding to the maximum of curvature, with a progressive increase of the gates widths at the sides of the identified maximum. The upper colored bar in Fig. 8 show the gate widths determined by our adaptive-gating scheme while the lower bar shows those defined in the log-gating scheme; the colors correspond to the gate-width. Our adaptive scheme departs from the previous log-gating only near the maxima of the transient curvature. The gate-width is smaller with respect to the log-gating scheme in correspondence to blue or light-blue colors, while is slightly greater at their sides (red bars in Fig. 8).

The data sampled with both the adaptive-gating and log-gating schemes were inverted with AarhusInv inversion code (Kirkegaard and Auken, 2015).

The results of individual inversions depend significantly on the random noise present in the data and this can overprint the effect of the type of sampling used, preventing us from getting a unique conclusion on the validity of our new approach to sampling the EM transient.

To overcome this problem we decided to conduct our study with a probabilistic approach. We carried out 1000 inversions with adaptive-gating configuration and 1000 inversions with log-gating configuration, considering 1000 different random noise realizations.

In this way, our results are independent from a specific random noise, but depend only on the gating scheme that we used.

The Fig. 9 synthesizes all the steps that we conducted for the considered four-layer models.

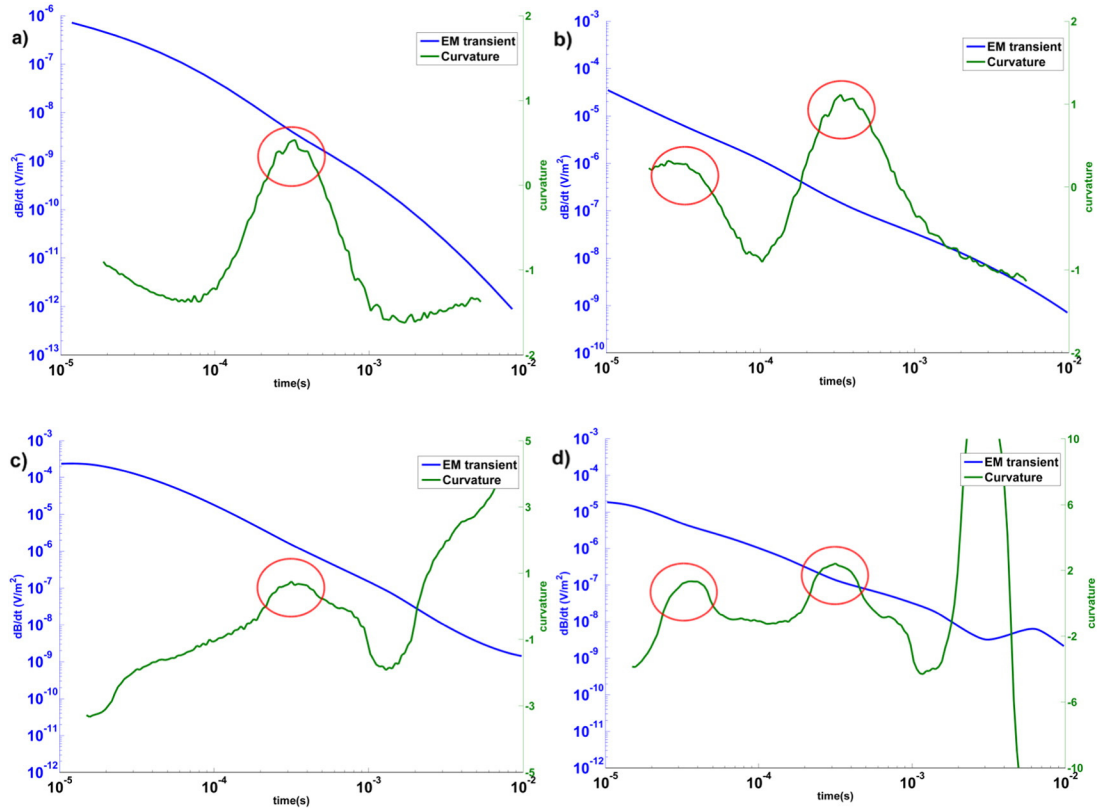

Fig. 7. Comparison, for the first and the second four-layer model earth, between the identified maxima of curvature for free-noise data (a and b) and filtered data through DWT (c and d).

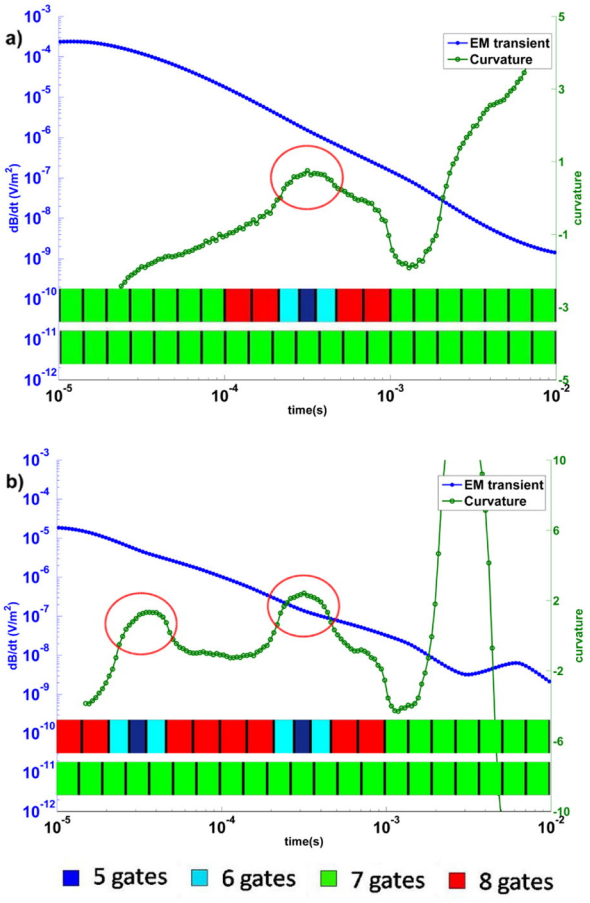

Fig. 8. (a) EM filtered transient (blue curve) and its curvature (green curve) for the first four-layer model earth; (b) EM filtered transient (blue curve) and its curvature (green curve) for the second four-layer model earth. The dashed circles mark the maxima of curvature. The lower and upper colored bars indicate the width of the gates for log-gating adaptive-gating schemes, respectively. The colors correspond to the gate-width. (For interpretation of the references to color in this figure legend, the reader is referred to the web version of this article.)

From the 1000 inversion models for both sampling schemes, we calculated an average inverse model and compared the results with the true models. The results for the two four-layer models are shown in Figs. 10 and 11, where the true model (blue curve), the average model (black curve) and the 1000 inverse models (red curves) are plotted in the depth/resistivity space.

As we can clearly see from Fig. 10, the adaptive gating, detailing the sampling at the maximum of the curvature (Fig. 8a), allows the inversion to recover more accurate information on the resistivity and the thickness of the third layer, with respect to the log-gating.

The results are similar also for the second four-layer model. In this case, the second derivative showed two maxima of curvature (Fig. 8b), marking the transition, respectively, between the first and the second layer, and the third and the fourth layer (Fig. 11).

A closer inspection of the scattering of the individual models also reveals that the adaptive gating provides, in general, more precise results (i.e., closer to true model, smaller dispersion and standard deviation) across all layers. In fact, based on the 1000 inversion models, for both four-layer models, we also carried out a study on the precision of the recovered model parameters. In particular, we calculated the standard deviation, as percentage, associated with the resistivities and the thicknesses of the average models. The results are listed in Table 2:

As we can see, the parameters obtained using the adaptive-gating scheme are more precise than those in log-gating scheme.

3.2. Buried valley model

The next experiment is related to a simulation of the field data from a buried valley structure. All the steps in the previous section were independently applied for each of the 52 soundings in this simulation. That is, the time of the gates varies across the 2D model. For each sounding, we calculated an average model from the 1000 inversions in both adaptive-gating and log-gating scheme. The plotted results refer to the 52 average models obtained with the two tested sampling schemes (Fig. 12). The adaptive-gating allowed us to recover with more accuracy the geometry of the buried valley (Fig. 12b). The thicknesses of the second and the third layer are better defined than in the log-gating case,

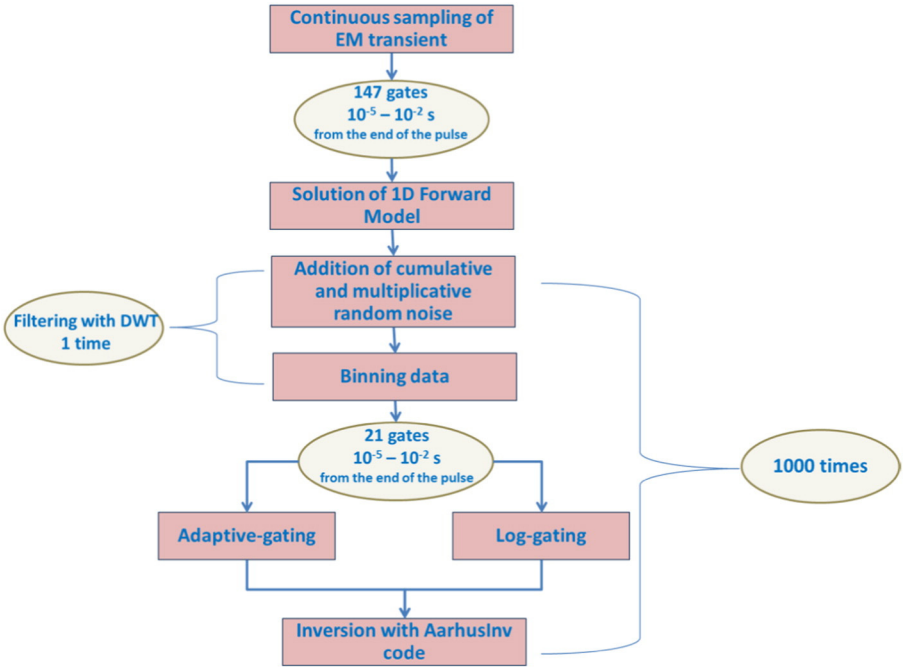

Fig. 9. All the steps of our workflow to make comparison between adaptive-gating and log-gating.

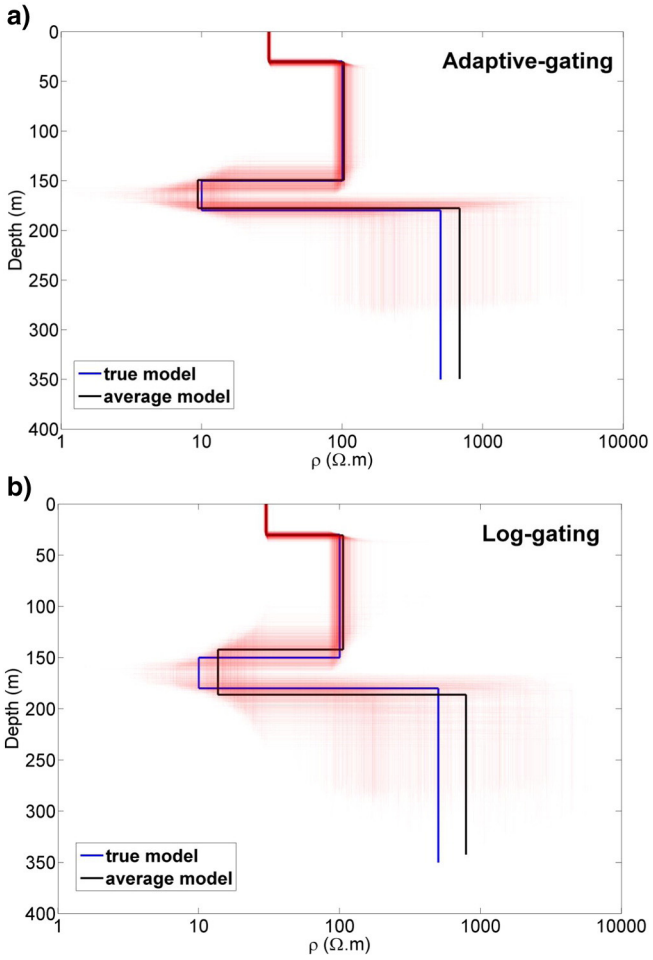

Fig. 10. True model (blue curve), average model (black curve), 1000 inverse models (red curves) for the first four-layer model obtained with adaptive-gating (a) and log-gating (b) schemes. (For interpretation of the references to color in this figure legend, the reader is referred to the web version of this article.)

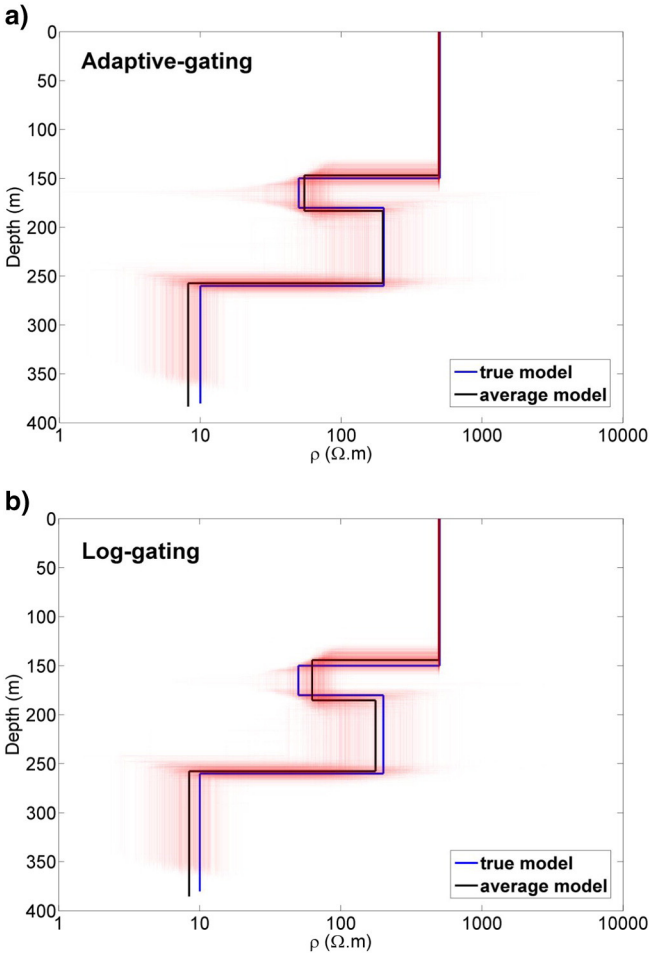

Fig. 11. True model (blue curve), average model (black curve), 1000 inverse models (red curves) for the second four-layer model obtained with adaptive-gating (a) and log-gating (b) schemes. (For interpretation of the references to color in this figure legend, the reader is referred to the web version of this article.)

especially when the depth of the third layer is greater than 120 m. At the sides of the section, where the third conductive layer is located at shallow depth, both configurations give correct results and its geometry is correctly retrieved. Conversely, when the depth to the third layer increases, the classical log-gating of the EM transient can lead to considerable errors on both resistivity and thickness of the third layer (Fig. 12d). For each average model, we calculated also the data residual defined as (Auken and Christiansen, 2004): from the Fig. 12c and e we can see that the values are similar for both gating schemes and every model fits the data within the noise level.

Based on the 1000 performed inversions we also carried out a study on the precision of the model parameters recovered. In particular, we calculated the standard deviation associated with the resistivity (Fig. 13) and the thickness (Fig. 14) of average models.

In general, the standard deviation of the resistivity decreases in the central soundings, while the standard deviation of the thickness increases for the same soundings. However, for both parameters, the standard deviation is lower for the models obtained by using the adaptive-gating scheme.

In conclusion, by sampling the EM transient with the adaptive-gating scheme we obtain inverse models that are more accurate (Fig. 12), more precise (Figs. 13 and 14) than standard sampling scheme. These results yield overall more reliable information on the resistivity structures of the subsurface.

4. Discussion

From the shown examples, it is evident that the adaptive gating technique allows to solve accurately the geometry of the subsurface structures. Considering the example of a buried 2D valley, the depth and the thickness of the electro-layers are better determined by our technique than by standard methods. Although this structure can be considered a rather common one in hydrogeological applications, we expect good results also in the case of structures typical of other areas of exploration (e.g.: oiltrap structures).

The results shown were obtained by considering the changes of slope in transient electromagnetic related to resistivity contrasts between the layers in the subsurface and defining a detailed sampling in correspondence of the maximum of curvature which mark the transition between resistive layers to conductive layers. However, similar variations of shape, and then variation of slope, within an electromagnetic transient, may also be due to other effects, not taken into account in this work, such as the effects of the low-pass filter at the receivers or the presence of highly polarizable bodies that can lead to induced polarization phenomena. It is expected that applying the adaptive gating also to these effects would be beneficial to a more accurate sampling and modeling of these effects. This in turn will provide better recovery of the resistivity distribution in the subsurface.

As we have shown, using adaptive-gating can improve the accuracy of the recovered models.

Table 2
Standard deviation as percentage of the value of the model parameters obtained with adaptive-gating and log-gating schemes for both four-layer models used in this simulation.

	First four-layer model				Second four-layer model			
	Adaptive-Gating		Log-gating		Adaptive-Gating		Log-gating	
	Resistivity (%)	Thickness (%)	Resistivity (%)	Thickness (%)	Resistivity (%)	Thickness (%)	Resistivity (%)	Thickness (%)
1° layer	1	6	1	7	1	5	1	5
2° layer	11	8	48	11	25	17	28	18
3° layer	28	15	40	30	78	8	90	8.7
4° layer	93		122		36		38	

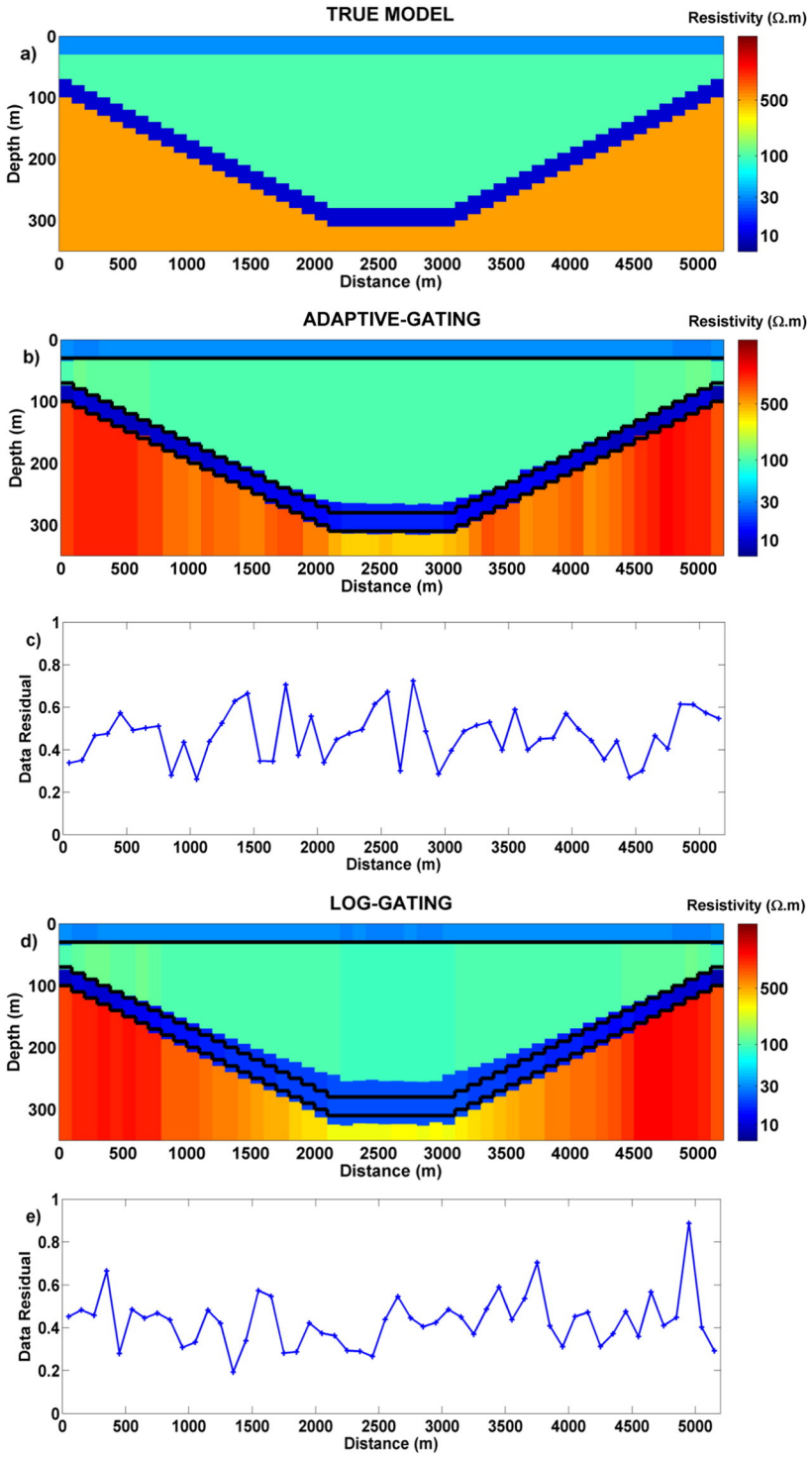

Fig. 12. (a) True buried valley model. Buried valley model obtained with adaptive-gating (b) and log-gating (d) schemes. Data residual for each average model using adaptive-gating (c) and log-gating (e) configuration.

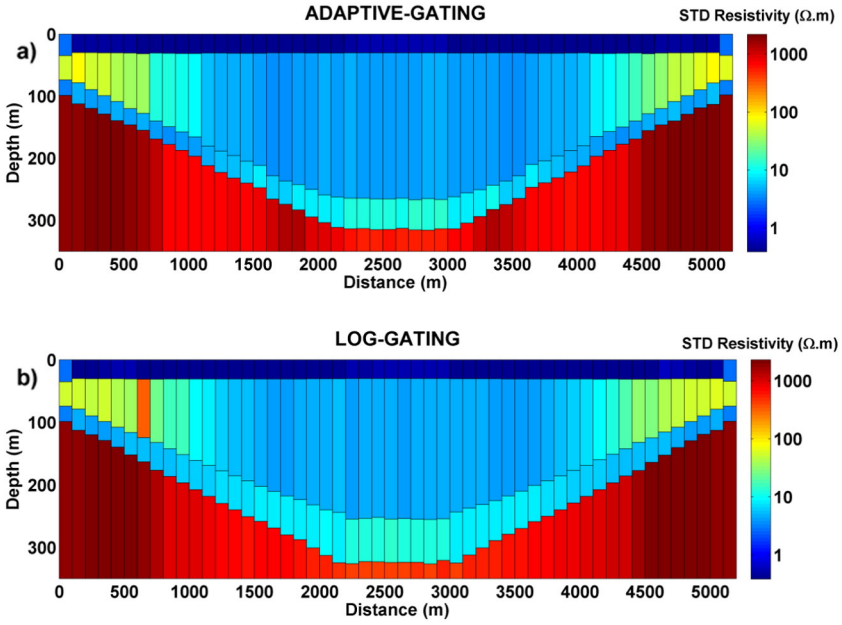

Fig. 13. Standard deviation associated with the resistivity of the average inverse models for adaptive-gating (a) and log-gating (b) schemes.

Our approach simply departs from the log-gating, adding or removing one or two gates in correspondence the maxima of the transient curvature (Fig. 8) to get the new binned scheme. In our cases, this imply a decrease of the 20–30% of the gate widths at the maximum of curvature, compared with those in log-gating scheme. These values may vary depending on some dataset characteristics (e.g., sampling rate, etc.), but we expect that the optimum value should not depart significantly from this figure.

We do however realize that in real AEM data, some post-processing filtering procedures are often applied to the acquired data (e.g., leveling or bias removal). Such procedures usually require constant sampling scheme of the transients, and are therefore probably unsuitable for completely unconstrained adaptive gating. This may imply that the right compromise might be found in slowly varying adaptive gate times.

On a related note, another reason for not applying the same log-gating throughout a given AEM survey is given by the fact that the overall S/N ratio might, and usually does, vary across the survey area. Reasons vary from the presence of noisier background areas (natural or man-made activities) to varying geology (varying secondary signal), to varying AEM system altitude (e.g., higher flying height due to forested areas). It would be worth considering customized gating for each one of these areas, based on the local S/N conditions, with the aim of using best the gates. For example, in places where the signal drops into noise early in the transient, it would be beneficial to move most of the gates above the noise level (albeit narrowing them).

5. Conclusions

We have presented a new approach for defining a gating scheme for the sampling of the AEM data obtained from modern airborne EM systems. Instead of defining a priori the type of gating (such as log-gating) and the characteristics of the gating of the different channels

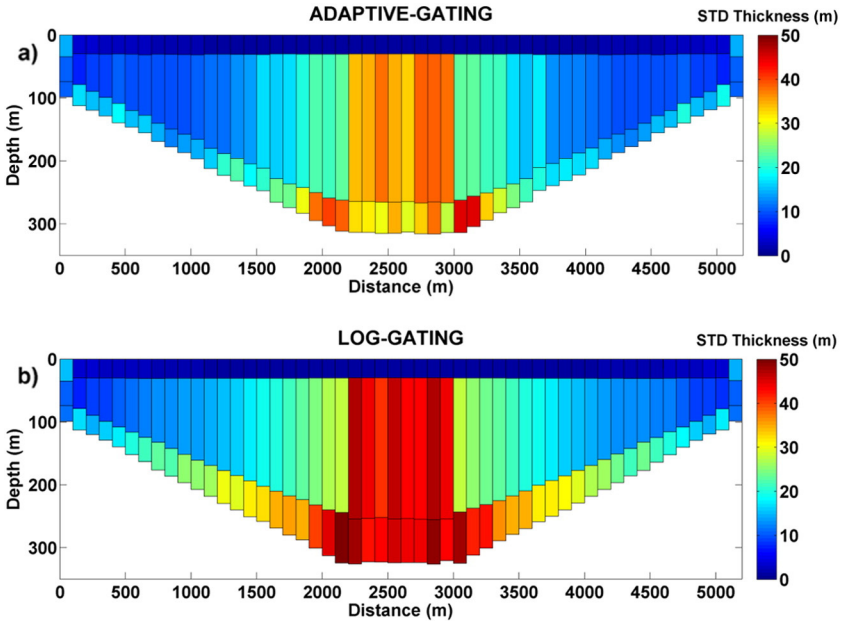

Fig. 14. Standard deviation associated with the thickness of the average inverse models for adaptive-gating (a) and log-gating (b) schemes.

(center times, width), we showed that it may be advantageous to define a priori only the maximum number of channels to use, and place them adaptively across the transient.

The method is based on sampling the EM transient decay in a more detailed way in correspondence of the maxima of the curvature of the data, marking the transition from a resistive layer to a conductive one. The adaptive-gating scheme consists in reducing the width of the gate in correspondence of the maxima of the curvature and increasing the width of the adjacent gates at its sides in a progressive way.

However, the computation of the second derivative of the EM transient enhances excessively the noise contained in the signal, so our method necessarily involves a preliminary low-pass filter.

We chose to use a technique based on Discrete Wavelet Transform that allows performing a localized denoising. The study of synthetic data allowed us to verify that the DWT is a suitable filtering technique for this type of signal. This leads us to consider the possibility of using DWT during processing of AEM data.

The improvements in both the accuracy and precision of the estimated parameters of the inverse models obtained with the adaptive-gating scheme, confirm the validity of the idea of adapting the sampling of the EM transient to the specific characteristics of the data.

Although our study was conducted on synthetic data, the results have been very encouraging and have demonstrated that an adaptive sampling of the EM transient can produce more correct inverse resistivity models, and subsequent interpretations.

In this paper we didn't investigate a way to automate this procedure. However, we think that some ideas to automate the denoising of the second derivative and the selection of its maxima could be implemented.

To denoise the data with DWT we could choose to filter a fixed number of scales for all the survey. The scales to be filtered could be checked by a preliminary analysis of a selection of soundings from different areas of the survey. As about the identification of the maxima, we think that some criteria involving an amplitude threshold of the maxima and excluding the late times, when the S/N ratio is evidently low, may be applied with success or even a combined study of the first and the second derivative of the EM transient.

We demonstrated the validity of our technique when applied to 1D cases. We plan to investigate under which conditions this approach, or parts thereof, can be applied successfully in more complex 2D or 3D cases.

Acknowledgements

We would like to thank the editor Jonathan Chambers, the reviewer Jacques Desmarais and an anonymous reviewer for their comments that helped to improve and clarify parts of the paper.

References

Auken, E., Christiansen, A.V., 2004. Layered and laterally constrained 2D inversion of resistivity data. Geophysics 69, 752–761.
Auken, E., Jørgensen, F., Sørensen, K.I., 2003. Large-scale TEM investigation for groundwater. Explor. Geophys. 33, 188–194.
Christiansen, A.V., Auken, E., Sørensen, K., 2009. The transient electromagnetic method in groundwater geophysics. Springer Berlin Heidelberg, pp. 179–226.
Fedi, M., Quarta, T., 1998. Wavelet analysis for the regional-residual and local separation of potential field anomalies. Geophys. Prospect. 46, 507–525.
Fitterman, D.V., 1987. Examples of transient sounding for groundwater exploration in sedimentary aquifers. Ground Water 25, 684–693.
Kirkegaard, C., Auken, E., 2015. A parallel, scalable and memory efficient inversion code for very large-scale airborne. EM Sur.: Geophys. Prospect. 63, 495–507.
Munkholm, M.S., Auken, E., 1996. Electromagnetic noise contamination on transient electromagnetic soundings in culturally disturbed environments. Eur. J. Environ. Eng. Geophys. 1, 119–127.
Nabighian, M.N., Macnae, J.C., 1991. In: Nabighian, M.N. (Ed.), Appendix A: TEM systems, in Electromagnetic methods in applied geophysics — application. SEG publication, pp. 479–483.
Podgorski, J.E., Auken, E., Schamper, C., Christiansen, A.V., Kalscheuer, T., Green, A.G., 2013. Processing and inverting commercial helicopter time-domain electromagnetic data for environmental assessments and geological and hydrological mapping. Geophysics 78, E149–E159.
Reid, J.E., Viezzoli, A., 2007. High-resolution near surface airborne electromagnetics—SkyTEM survey for uranium exploration at Pells Range, WA. 19th Geophysical Conference and Exhibition. Australian Society of Exploration Geophysicists (Extended Abstracts).
Telford, W.M., Geldart, L.P., Sheriff, R.A., 1990. Applied Geophysics. 2nd edition. Cambridge Univ. Press.
Viezzoli, A., Tosi, L., Teatini, P., Silvestri, S., 2010. Surface water–groundwater exchange in transitional coastal environments by airborne electromagnetics: the Venice Lagoon example. Geophys. Res. Lett. 37, L01402 (6 pp).
Ward, S.H., Hohmann, G.W., 1988. In: Nabighian, M.N. (Ed.), Electromagnetic theory for geophysical applications, in Electromagnetic Methods in Applied Geophysics — Theory vol. 1. SEG publication, pp. 131–311.